

Journal of Visualized Experiments

Fabrication of Ti3C2 MXene Microelectrode Arrays for In Vivo Neural Recording --Manuscript Draft--

Article Type:	Invited Methods Article - JoVE Produced Video
Manuscript Number:	JoVE60741R1
Full Title:	Fabrication of Ti3C2 MXene Microelectrode Arrays for In Vivo Neural Recording
Section/Category:	JoVE Bioengineering
Keywords:	MXene; two-dimensional materials; nanomaterials; bioelectronics; neural microelectrodes; neural interfaces; neuroengineering
Corresponding Author:	Flavia Vitale UNITED STATES
Corresponding Author's Institution:	
Corresponding Author E-Mail:	vitalef@pennmedicine.upenn.edu
Order of Authors:	Nicolette Driscoll Kathleen Maleski Andrew G. Richardson Brendan Murphy Babak Anasori Timothy H. Lucas Yury Gogotsi Flavia Vitale
Additional Information:	
Question	Response
Please indicate whether this article will be Standard Access or Open Access.	Standard Access (US\$2,400)
Please indicate the city, state/province, and country where this article will be filmed . Please do not use abbreviations.	Philadelphia, PA, USA



Departments of Neurology, Physical Medicine & Rehabilitation
Center for Neuroengineering and Therapeutics
Perelman School of Medicine, University of Pennsylvania

Flavia Vitale, Ph.D.
Assistant Professor

Center for Neurotrauma, Neurodegeneration & Restoration
Philadelphia VA Medical Center

August 30th, 2019
To: Nandita Singh, PhD
Senior Science Editor
Journal of Visualized Experiments

Dear Nandita,

We are pleased to submit our manuscript, **"Fabrication of Ti_3C_2 MXene microelectrode arrays for *in vivo* neural recording"**, for consideration in the *Journal of Visualized Experiments*. Our paper describes a method for fabricating multichannel Ti_3C_2 MXene microelectrode arrays for high-resolution recording of neural activity.

There is tremendous interest among the neuroscience community in developing novel tools for mapping neural activity and elucidating the fundamental mechanisms underlying brain diseases and disorders, which typically occur on the submillimeter scale in brain microcircuits. However, the lack of materials which can form a stable, low-impedance, biocompatible interface with brain tissue while allowing the use of simple, scalable fabrication methods has so far limited the development of high-fidelity neural interfaces. Ti_3C_2 MXene is a recently discovered two-dimensional nanomaterial combining high electrical conductivity and capacitance with hydrophilic surface properties that are unique among other carbon-based nanomaterials. Our group has previously shown that Ti_3C_2 MXene microelectrodes are exquisitely sensitive for recording neuronal activity and exhibit remarkably low interface impedance. In this work, we describe the process for synthesizing high quality Ti_3C_2 MXene, and utilizing high-throughput solution processing methods to fabricate microscale, high-resolution neural electrode arrays of Ti_3C_2 MXene. We also detail methods for connecting these electrode arrays to a data acquisition system and performing *in vivo* recording experiments. We hope that this protocol will serve as a guide and offer a simpler and more scalable method for fabricating microelectrodes from Ti_3C_2 MXene or other conductive inks than methods that are currently available.

Please do not hesitate to contact us if we can provide any further information. We look forward to your response.

Sincerely,

A handwritten signature in black ink, appearing to read "Flavia Vitale".

Flavia Vitale, Ph.D.
Assistant Professor
Department of Neurology
Center for Neuroengineering and Therapeutics
University of Pennsylvania
Philadelphia, PA

TITLE:**Fabrication of Ti_3C_2 MXene Microelectrode Arrays for *In Vivo* Neural Recording****AUTHORS AND AFFILIATIONS:**

Nicolette Driscoll^{1,2,3}, Kathleen Maleski^{4,5}, Andrew G. Richardson^{2,6}, Brendan Murphy^{1,2,3}, Babak Anasori^{4,5}, Timothy H. Lucas^{2,6}, Yury Gogotsi^{4,5}, Flavia Vitale^{1,2,3,7,8}

¹Department of Bioengineering, University of Pennsylvania, Philadelphia, PA, USA

²Center for Neuroengineering and Therapeutics, University of Pennsylvania, Philadelphia, PA, USA

³Corporal Michael J. Crescenz Veterans Affairs Medical Center, Philadelphia, PA, USA

⁴Department of Materials Science and Engineering, Drexel University, Philadelphia, PA, USA

⁵A.J. Drexel Nanomaterials Institute, Drexel University, Philadelphia, PA, USA

⁶Department of Neurosurgery, University of Pennsylvania, Philadelphia, PA, USA

⁷Department of Neurology, University of Pennsylvania, Philadelphia, PA, USA

⁸Department of Physical Medicine and Rehabilitation, Philadelphia, PA, USA

Corresponding Author:

Flavia Vitale (vitalef@pennmedicine.upenn.edu)

Email Addresses of Co-Authors:

Nicolette Driscoll (ndris@seas.upenn.edu)

Kathleen Maleski (kam645@drexel.edu)

Andrew G. Richardson (Andrew.Richardson@pennmedicine.upenn.edu)

Brendan Murphy (bremu@seas.upenn.edu)

Babak Anasori (banasori@iupui.edu)

Timothy H. Lucas (Timothy.Lucas@pennmedicine.upenn.edu)

Yury Gogotsi (yg36@drexel.edu)

Flavia Vitale (vitalef@pennmedicine.upenn.edu)

KEYWORDS:

MXene, two-dimensional materials, nanomaterials, bioelectronics, neural microelectrodes, neural interfaces, neuroengineering

SUMMARY:

We describe here a method for fabricating Ti_3C_2 MXene microelectrode arrays and utilizing them for *in vivo* neural recording.

ABSTRACT:

Implantable microelectrode technologies have been widely used to elucidate neural dynamics at the microscale to gain a deeper understanding of the neural underpinnings of brain disease and injury. As electrodes are miniaturized to the scale of individual cells, a corresponding rise in the interface impedance limits the quality of recorded signals. Additionally, conventional electrode materials are stiff, resulting in a significant mechanical mismatch between the electrode and the

surrounding brain tissue, which elicits an inflammatory response that eventually leads to a degradation of the device performance. To address these challenges, we have developed a process to fabricate flexible microelectrodes based on Ti_3C_2 MXene, a recently discovered nanomaterial that possesses remarkably high volumetric capacitance, electrical conductivity, surface functionality, and processability in aqueous dispersions. Flexible arrays of Ti_3C_2 MXene microelectrodes have remarkably low impedance due to the high conductivity and high specific surface area of the Ti_3C_2 MXene films, and they have proven to be exquisitely sensitive for recording neuronal activity. In this protocol, we describe a novel method for micropatterning Ti_3C_2 MXene into microelectrode arrays on flexible polymeric substrates and outline their use for *in vivo* micro-electrocorticography recording. This method can easily be extended to create MXene electrode arrays of arbitrary size or geometry for a range of other applications in bioelectronics and it can also be adapted for use with other conductive inks besides Ti_3C_2 MXene. This protocol enables simple and scalable fabrication of microelectrodes from solution-based conductive inks, and specifically allows harnessing the unique properties of hydrophilic Ti_3C_2 MXene to overcome many of the barriers that have long hindered the widespread adoption of carbon-based nanomaterials for high-fidelity neural microelectrodes.

INTRODUCTION:

Understanding the fundamental mechanisms underlying neural circuits, and how their dynamics are altered in disease or injury, is a critical goal for developing effective therapeutics for a broad range of neurological and neuromuscular disorders. Microelectrode technologies have been widely used to elucidate neural dynamics on fine spatial and temporal scales. However, obtaining stable recordings with high signal-to-noise ratio (SNR) from microscale electrodes has proven to be particularly challenging. As the dimensions of the electrodes are reduced to approach cellular scale, a corresponding rise in electrode impedance degrades signal quality¹. Additionally, numerous studies have shown that rigid electrodes comprised of conventional silicon and metal electronic materials produce significant damage and inflammation in the neural tissue, which limits their usefulness for long-term recording²⁻⁵. Given these facts, there has been significant interest in developing microelectrodes with new materials which can reduce the electrode-tissue interface impedance and can be incorporated into soft and flexible form factors.

One commonly used method for reducing the electrode-tissue interface impedance is increasing the area over which ionic species in the extracellular fluid can interact with the electrode, or the “effective surface area” of the electrode. This can be achieved through nanopatterning⁶, surface roughening⁷, or electroplating with porous additives^{8,9}. Nanomaterials have gained significant attention in this field because they offer intrinsically high specific surface areas and unique combinations of favorable electrical and mechanical properties¹⁰. For example, carbon nanotubes have been used as a coating to significantly reduce electrode impedance¹¹⁻¹³, graphene oxide has been processed into soft, flexible free-standing probe electrodes¹⁴, and laser-pyrolyzed porous graphene has been utilized for flexible, low-impedance micro-electrocorticography (micro-ECOG) electrodes¹⁵. Despite their promise, a lack of scalable assembly methods has limited the widespread adoption of nanomaterials for neural interfacing electrodes. Carbon-based nanomaterials in particular are typically hydrophobic, and thus require the use of surfactants¹⁶, superacids¹⁷, or surface functionalization¹⁸ to form aqueous dispersions

for solution-processing fabrication methods, while alternative methods of fabrication, such as chemical vapor deposition (CVD), typically require high temperatures which are incompatible with many polymeric substrates^{19–22}.

Recently, a class of two-dimensional (2D) nanomaterials, known as MXenes, has been described which offers an exceptional combination of high conductivity, flexibility, volumetric capacitance, and inherent hydrophilicity, making them a promising class of nanomaterials for neural interfacing electrodes²³. MXenes are a family of 2D transition metal carbides and nitrides which are most commonly produced by selectively etching the A element from layered precursors. These are typically MAX phases with the general formula $M_{n+1}AX_n$, where M is an early transition metal, A is a group 12–16 element of the periodic table, X is carbon and/or nitrogen, and $n = 1, 2$, or 3 ²⁴. Two-dimensional MXene flakes have surface-terminating functional groups that can include hydroxyl (–OH), oxygen (–O) or fluorine (–F). These functional groups make MXenes inherently hydrophilic and enable flexible surface modification or functionalization. Of the large class of MXenes, Ti_3C_2 has been the most extensively studied and characterized^{25–27}. Ti_3C_2 shows remarkably higher volumetric capacitance ($1,500\text{ F/cm}^3$)²⁸ than activated graphene ($\sim 60\text{--}100\text{ F/cm}^3$)²⁹, carbide-derived carbons (180 F/cm^3)³⁰, and graphene gel films ($\sim 260\text{ F/cm}^3$)³¹. Furthermore, Ti_3C_2 shows extremely high electronic conductivity ($\sim 10,000\text{ S/cm}$)³², and its biocompatibility has been demonstrated in several studies^{33–36}. The high volumetric capacitance of Ti_3C_2 films is advantageous for biological sensing and stimulation applications, because electrodes that exhibit capacitive charge transfer can avoid potentially harmful hydrolysis reactions.

Our group has recently demonstrated flexible, thin-film Ti_3C_2 microelectrode arrays, prepared using solution processing methods, which are capable of recording both micro-electrocorticography (micro-ECoG) and intracortical neuronal spiking activity *in vivo* with high SNR³⁶. These MXene electrodes showed significantly reduced impedance compared to size-matched gold (Au) electrodes, which can be attributed to the high conductivity of MXene and the high surface area of the electrodes. In this protocol, we describe the key steps for fabricating planar microelectrode arrays of Ti_3C_2 MXene on flexible parylene-C substrates and utilizing them *in vivo* for intraoperative micro-ECoG recording. This method takes advantage of the hydrophilic nature of MXene, which makes possible the use of solution processing methods that are simple and scalable while not requiring the use of surfactants or superacids to achieve stable aqueous suspensions. This ease of processability may enable cost-effective production of MXene biosensors at industrial scales, which has been a major limitation to the widespread adoption of devices based on other carbon nanomaterials. The key innovation in the electrode fabrication lies in the use of a sacrificial polymeric layer to micropattern the MXene after spin-coating, a method adapted from literature on solution-processed poly(3,4-ethylenedioxythiophene):poly(styrene sulfonate) (PEDOT:PSS) microelectrodes³⁷, but which had not previously been described for patterning MXene. The exceptional electrical properties of Ti_3C_2 , coupled with its processability and 2D morphology make it a very promising material for neural interfaces. In particular, Ti_3C_2 offers a route towards overcoming the fundamental trade-off between electrode geometric area and electrochemical interface impedance, a primary limiting factor for micro-scale electrode performance. Additionally, the fabrication procedure

described in this protocol can be adapted to produce MXene electrode arrays of varying sizes and geometries for different recording paradigms, and can also easily be adapted to incorporate other conductive inks besides MXene.

PROTOCOL:

All *in vivo* procedures conformed to the National Institutes of Health (NIH) Guide for the Care and Use of Laboratory Animals and were approved by the Institutional Animal Care and Use Committee (IACUC) of the University of Pennsylvania.

1. Synthesis of Ti_3C_2 MXene

NOTE: The reaction procedures described in this section are intended for use inside a chemical fume hood. Washing steps included in this procedure are intended to be used with balanced centrifuge tubes. All waste produced is considered hazardous waste and should be discarded appropriately following University guidelines.

CAUTION: Hydrofluoric acid (HF) is an extremely dangerous, highly corrosive acid. Consult the materials safety data sheets (MSDS) for the chemicals used to synthesize MXenes before use and implement and follow appropriate safety measures. Appropriate personal protective equipment (PPE) for handling HF includes a laboratory coat, acid resistant apron, close-toed shoes, long pants, goggles, full face shield, nitrile gloves, and HF resistant gloves made of butyl rubber or neoprene rubber.

1.1. MAX phase synthesis

1.1.1. Synthesize Ti_3AlC_2 by ball milling TiC (2 μm), Ti (44 μm), and Al (44 μm) powders at a molar ratio (TiC:Ti:Al) of 2:1:1 for 18 h using zirconia balls. Place the powders in an alumina crucible, heat to 1,380 $^{\circ}\text{C}$ (5 $^{\circ}\text{C}$ heating rate) and hold for 2 h under argon. After the powders have been cooled, mill the MAX block and sieve through a 200 mesh sieve (<74 μm particle size).

NOTE: The Ti_3AlC_2 MAX phase precursor used to synthesize MXenes has been shown to have direct implications on the resulting Ti_3C_2 MXene properties³⁸. The Ti_3C_2 used to fabricate neural electrodes was selectively etched from MAX prepared following a previous procedure²⁶.

1.2. Etching: Removal of the Al layer in Ti_3AlC_2 in an acidic etchant solution (Figure 1A)

1.2.1. Prepare the selective etching solution in a 125 mL plastic container by first adding 12 mL of deionized water (DI H_2O) followed by the addition of 24 mL of hydrochloric acid (HCl). Wearing all appropriate HF etching PPE, add 4 mL of HF to the etchant container. Perform selective etching by slowly adding 2 g of Ti_3AlC_2 MAX phase to the reaction container and stirring with a Teflon magnetic bar for 24 h at 35 $^{\circ}\text{C}$ at 400 rpm.

1.3. Washing: Bringing the material to neutral pH.

1.3.1. Fill two 175 mL centrifuge tubes with 100 mL of DI H₂O. Split the etching reaction mixture into 175 mL centrifuge tubes and wash the material by repeated centrifugation at 3,500 rpm (2,550 x g) for 5 min. Decant the acidic supernatant into a plastic hazardous waste container. Repeat until the pH reaches 6.

1.4. Intercalation: Insertion of molecules between multilayer MXene particle to waken out-of-plane interactions (**Figure 1B**)

1.4.1. Add 2 g of lithium chloride (LiCl) to 100 mL of DI H₂O and stir at 200 rpm until dissolved. Mix 100 mL of LiCl/H₂O with the Ti₃C₂/Ti₃AlC₂ sediment and stir the reaction for 12 h at 25 °C.

1.5. Delamination: Exfoliation from bulk multilayer particle into single- to few- layer Ti₃C₂ MXene (**Figure 1C**)

1.5.1. Wash the intercalation reaction in 175 mL centrifuge tubes by centrifugation at 2,550 x g for 5 min. Decant the clear supernatant. Repeat until a dark supernatant is found.

1.5.2. Continue to centrifuge for 1 h at 2,550 x g. Decant the dilute-green supernatant.

1.5.3. Re-disperse the swollen sediment with 150 mL of DI H₂O. Transfer supernatant to 50 mL centrifuge tubes and centrifuge at 2,550 x g for 10 min to separate remaining MAX (sediment) from MXene (supernatant).

NOTE: Re-dispersion of the sediment will become difficult and will require agitation or manual shaking.

1.5.4. Collect supernatant as Ti₃C₂ MXene. Perform further size selection and optimization of the solution to isolate single- to few-layer flakes by collecting the supernatant following a centrifugation step at 2,550 x g for 1 h.

1.6. Solution storage: Packaging the MXene ink for long-term storage (**Figure 1D**)

1.6.1. Argon bubble the solutions for 30 min prior to packaging in an Argon sealed headspace vial (transfer via a syringe). Store solutions at high concentrations (>5 mg/mL), away from sunlight, and at low temperatures (≤5 °C) to ensure longevity.

2. Fabrication of Ti₃C₂ MXene microelectrode arrays

NOTE: The procedure described in this section is intended for use inside a standard university clean room facility, such as the Singh Center for Nanotechnology at the University of Pennsylvania. This facility, as well as similar facilities, are accessible to outside users as part of the National Nanotechnology Infrastructure Network (NNIN) supported by the National Science Foundation (NSF). In these facilities, many of the tools, equipment, and materials described in

this section are provided along with access to the clean room facility and would not require separate purchase.

CAUTION: Many of the chemicals used in the fabrication of MXene electrodes are hazardous, including photoresists, RD6 developer, remover PG, aluminum etching solution, and buffered oxide etchant. Consult MSDS for these chemicals before use and implement and follow appropriate safety measures at all times. All chemicals should be handled in a fume hood.

2.1. Deposit a 4 μm thick bottom layer of parylene-C onto a clean Si wafer (see **Figure 2A**).

2.2. Use the first photomask (mask-1) to define the metal interconnects of the devices, as well as a metal ring around the edge of the wafer to aid in later lift-off steps (**Figure 2B**).

2.2.1. Spin coat NR71-3000p onto the wafer at 3,000 rpm for 40 s. Soft bake the wafer on a hot plate for 14.5 min at 95 $^{\circ}\text{C}$.

2.2.2. Load the wafer and mask-1 into a mask aligner. Position the wafer so that the ring on the photomask overlaps with all edges of the wafer.

2.2.3. Expose with i-line (365 nm wavelength) at a dose of 90 mJ/cm². Hard bake the wafer on a hot plate for 1 min at 115 $^{\circ}\text{C}$.

2.2.4. Immerse the wafer in the RD6 developer for 2 min, continuously agitating the solution. Rinse thoroughly with DI H₂O and blow dry with an N₂ gun.

2.2.5. Use an electron beam evaporator to deposit 10 nm Ti, followed by 100 nm Au onto the wafer.

NOTE: Typical deposition parameters are a base pressure of 5×10^{-7} Torr and a rate of 2 $\text{\AA}/\text{s}$.

2.2.6. Immerse the wafer in remover PG for ~ 10 min until the photoresist has dissolved and the excess metal has fully lifted off, leaving Ti/Au only in the desired interconnect traces and the ring around the edge of the wafer. Once lift-off appears complete, sonicate for 30 s to remove any remaining traces of unwanted metal. Rinse wafer first in clean remover PG solution, then thoroughly rinse in DI H₂O and dry the wafer with an N₂ gun.

2.3. Deposit the sacrificial parylene-C layer (**Figure 2C**).

2.3.1. Expose the wafer to O₂ plasma for 30 s to render the underlying parylene-C layer hydrophilic. Spin coat 2% cleaning solution (e.g., Micro-90) in DI H₂O onto the wafer at 1,000 rpm for 30 s. Allow wafer to air dry for at least 5 min.

NOTE: The dilute soap solution acts as an anti-adhesive, allowing the sacrificial parylene-C layer to be peeled up later in the process.

265
266 2.3.2. Deposit 3 μm of parylene-C onto the wafer.
267

268 2.4. Use the second photomask (mask-2) to define the MXene patterns and a ring around the
269 edge of the wafer (**Figure 2D**).
270

271 2.4.1. Repeat steps 2.2.1–2.2.4, this time using mask-2 and carefully aligning the alignment marks
272 between the wafer and photomask before exposure.
273

274 2.4.2. Use O_2 plasma reactive ion etching (RIE) to etch through the sacrificial parylene-C layer in
275 the areas not covered by the photoresist to define the MXene electrodes and traces, which
276 should partially overlap with the Ti/Au interconnects, as well as the ring around the edges of the
277 wafer. Confirm complete etching of the sacrificial parylene-C layer by using a profilometer to
278 measure the profile between the exposed Ti/Au interconnects and the bottom parylene-C layer.
279

280 NOTE: When etching is complete, the profile across the exposed metal surface will be smooth,
281 while the bottom parylene-C layer will be rough and partially etched. This etch step should be
282 completed in a planar etch RIE system, not a barrel asher, and etch times and parameters will be
283 highly dependent on the RIE system.
284

285 2.5. Spin-coat the MXene solution onto the wafer (**Figure 2E**).
286

287 2.5.1. Pipette MXene solution onto each of the desired MXene patterns, then spin the wafer at
288 1,000 rpm for 40 s. Dry the wafer on a 120 $^{\circ}\text{C}$ hot plate for 10 min to remove any residual water
289 from the MXene film.
290

291 2.6. Use an electron beam evaporator to deposit 50 nm SiO_2 onto the wafer, to act as a protective
292 layer over the MXene patterns for subsequent processing steps.
293

294 NOTE: Typical deposition parameters are a base pressure of 5×10^{-7} Torr and a rate of 2 $\text{\AA}/\text{s}$.
295

296 2.7. Remove the sacrificial parylene-C layer to pattern the MXene and SiO_2 layers (**Figure 2F**).
297

298 2.7.1. Apply a small drop of DI H_2O to the edge of the wafer and use tweezers to peel up the
299 sacrificial parylene-C layer, beginning where its edges are defined in the ring around the outside
300 of the wafer.
301

302 NOTE: The water will combine with the soap residue beneath the sacrificial parylene-C layer to
303 enable this lift-off.
304

305 2.7.2. Rinse the wafer thoroughly in DI H_2O to remove any remaining cleaning solution residue.
306 Dry the wafer with an N_2 gun, then place on a 120 $^{\circ}\text{C}$ hot plate for 1 h to remove any residual
307 water from the patterned MXene films.
308

2.8. Deposit the 4 μm thick top layer of parylene-C (**Figure 2G**).

2.9. Use the third photomask (mask-3) to define device outline and openings over electrodes and Au bonding pads (VIAs) (**Figure 2H**).

2.9.1. Repeat steps 2.2.1–2.2.4, this time using mask-3 and carefully aligning the alignment marks between the wafer and photomask before exposure.

2.9.2. Use an electron beam evaporator to deposit 100 nm Al onto the wafer.

NOTE: Typical deposition parameters are a base pressure of 5×10^{-7} Torr and a rate of 2 $\text{\AA}/\text{s}$.

2.9.3. Immerse the wafer in remover PG for ~ 10 min until the metal has fully lifted off, leaving Al covering the devices with openings for the electrodes and bonding pads. When lift-off is complete, sonicate for 30 s to remove any remaining traces of unwanted metal. Rinse wafer first in clean remover PG solution, then thoroughly rinse in DI H_2O and dry the wafer with an N_2 gun.

2.10. Etch the parylene-C to pattern the device outline and openings over electrodes and Au bonding pads (VIAs) (**Figure 2I**). Use O_2 plasma RIE to etch through the parylene-C layers surrounding the devices, and through the top parylene-C layer covering both the MXene electrode contacts and the Au bonding pads.

NOTE: Etching is complete when no parylene-C residue remains on the wafer between devices. The SiO_2 layer covering the MXene will act as an etch-stop layer, preventing the O_2 plasma from etching into or damaging the MXene electrode contacts.

2.11. Etch the Al layer covering the devices using a wet chemical etch in Al etchant type A at 50 $^\circ\text{C}$ either for 10 min, or for 1 min past when all visual traces of Al have disappeared, whichever comes first. Etch the SiO_2 covering the MXene electrodes using a wet chemical etch in 6:1 buffered oxide etchant (BOE) for 30 s (**Figure 2J**).

NOTE: The MXene microelectrode arrays are now complete.

2.12. Release the devices from the Si substrate wafer by placing a small drop of DI H_2O at the edge of a device, and gently peeling up the device as water is wicked underneath it by capillary action (**Figure 2K** and **Figure 3**).

3. Adapter construction and interfacing

NOTE: At this point, the thin film microelectrode arrays must be interfaced with an adapter to connect to the electrophysiology recording system. The 128ch stimulation/recording controller with the RHS2000 16-ch stim/record headstage (**Table of Materials**) used in this protocol requires input via a connector compatible with the 18-pin connector A79039-001. This section uses a printed circuit board (PCB, **Figure 4A**) with a zero-insertion force (ZIF) connector for interfacing

with the Au bonding pads on the microelectrode array and the connector A79040-001 for interfacing with the head-stage of the recording system. Depending on the data acquisition system, different connectors can be used on the PCB to enable interfacing with the electrophysiology headstage.

3.1. Solder the Omnetics and ZIF connectors to the PCB by applying a thin film of solder paste to each of the contact pads on the PCB, placing the parts in their appropriate locations, and heating on a hot plate until the solder reflows to form connections (**Figure 4B**).

NOTE: Reflow soldering can be done very easily on a hot plate or in a toaster oven and does not require the use of a costly reflow oven.

3.2. Apply two layers of polyimide tape (**Table of Materials**) to the back side of the Au bonding pad region of the MXene microelectrode array to give the device sufficient thickness to be secured in the ZIF connector. After applying the tape, trim any excess beyond the edges of the parylene-C device using a razor blade or precision scissors (**Figure 4C**).

3.3. Either under an inspection scope or using magnifying glasses, align the MXene microelectrode array in the ZIF connector so that the Au bonding pads align with the pins inside the ZIF connector, then close the ZIF to form a secure connection (**Figure 4D,E**).

NOTE: The ZIF connector used here is an 18-channel connector, while the device used here has 16 channels. The extra uncontacted channels are easily identified as an open circuit by means of impedance testing during recording sessions.

3.4. Test the electrochemical impedance of the MXene electrodes using a potentiostat to ensure successful fabrication and connection to the PCB adapter.

NOTE: Reasonable impedance values are given in the discussion section to aid in troubleshooting.

4. Acute implantation and neural recording

NOTE: Surgeries on adult male Sprague Dawley rats are performed using sterile instruments and with aseptic technique. Respiratory rate, palpebral reflex, and pedal pinch reflex are checked every 10 min to monitor depth of anesthesia. Body temperature is maintained with a heating pad.

4.1. Administer preemptive analgesia (subcutaneous injection of buprenorphine sustained release [SR], 1.2 mg/kg).

4.2. Administer anesthesia (intraperitoneal injection of a mixture of 60 mg/kg ketamine and 0.25 mg/kg dexmedetomidine).

4.3. Confirm proper level of anesthesia every 10 min throughout the experiment by checking for

absence of palpebral and pedal pinch reflexes.

4.4. Secure rat in stereotaxic frame, apply ocular lubricant to the eyes, and clean shaved scalp with 10% povidone-iodine.

4.5. Expose the calvaria with single midline scalp incision and blunt dissection of underlying tissue.

4.6. Place a 00-90 screw into the skull to serve as the ground for recordings.

4.7. Using a dental drill with a small burr, make a craniotomy at the desired cortical recording site.

4.8. Secure the array connector to a stereotaxic manipulator and position the device over the craniotomy. Gently lower until the entire array is in contact with the exposed cortex.

4.9. Wrap the ground wire around the skull screw.

4.10. Connect the recording system headstage to the array and begin recording spontaneous activity.

REPRESENTATIVE RESULTS:

Sample micro-ECoG data recorded on a MXene microelectrode array is shown in **Figure 5**. Following application of the electrode array onto the cortex, clear physiologic signals were immediately apparent on the recording electrodes, with approximately 1 mV amplitude ECoG signals appearing on all MXene electrodes. Power spectra of these signals confirmed the presence of two brain rhythms commonly observed in rats under ketamine-dexmedetomidine anesthesia: 1–2 Hz slow oscillations and γ oscillations at 40–70 Hz. Additionally, a signature broadband power attenuation during the “down” state of the slow oscillation, and selective β -band (15–30 Hz) and γ -band (40–120 Hz) power amplification during “up” state of the slow oscillation were observed. Results may vary based on the animal species used in the study, the targeted brain region, the anesthesia type, and the elapsed time since the administration of anesthesia.

FIGURE LEGENDS:

Figure 1: Schematic depicting MXene synthesis procedure. (A) Ti_3AlC_2 MAX is added to a selective etchant solution (HF, HCl, and DI H_2O), resulting in the removal of aluminum (Al). (B) After washing the etching solution to neutral pH using DI H_2O , multilayered Ti_3C_2 is obtained. Multilayered Ti_3C_2 is intercalated with Li^+ from an aqueous solution of lithium chloride (LiCl). (C) After washing the intercalation reaction, sediment swelling is observed representing the exchange of Li^+ with H_2O . Agitation of the swollen sediment results in exfoliated (or delaminated) single- to few-layer flakes of Ti_3C_2 MXene in H_2O . Size selection and separation of delaminated Ti_3C_2 MXene from multilayered Ti_3C_2 and Ti_3AlC_2 MAX phase occurs at this stage. (D) Ti_3C_2 MXene

ink is transferred via syringe to an Argon sealed headspace vial for long-term storage.

Figure 2: Schematics of the fabrication procedure for MXene microelectrode arrays. (A) Bottom parylene-C layer is deposited on a clean Si wafer. (B) Ti/Au (10 nm/100 nm) conductive traces are patterned through photolithography, e-beam deposition, and lift-off. (C) An anti-adhesive layer of 1% cleaning solution in DI H₂O is applied, followed by deposition of a sacrificial parylene-C layer. (D) The sacrificial parylene-C layer is patterned through photolithography and O₂ RIE etching. (E) Ti₃C₂ MXene is spin-coated onto the wafer, followed by e-beam deposition of 50 nm of SiO₂. (F) The sacrificial parylene-C layer is lifted off, residues of cleaning solution are rinsed off, and the wafer is baked dry. (G) Top parylene-C layer is deposited. (H) An Al etch mask layer is patterned through photolithography, e-beam deposition, and lift-off to define VIAs and device outline. (I) Parylene-C over electrode contacts and surrounding devices is etched away through O₂ RIE. (J) Al etch mask and SiO₂ protective layer over MXene are etched away through wet etch processes. (K) Finished device is lifted off wafer.

Figure 3: Photographs and optical microscopy images of MXene microelectrode arrays. (A) Photograph of a 3 inch Si wafer containing 14 completed MXene microelectrode arrays. Note the gold ring around the outer edge of the wafer, which is helpful for performing step 2.7 effectively. (B) Optical microscope image showing the peeling up of a completed device from the wafer using a small amount of DI H₂O. (C) Optical microscope image showing the array of MXene microelectrodes. (D) Optical microscope image of an individual MXene electrode. Scale bars, left to right: 1 cm, 3 mm, 500 μ m, 20 μ m.

Figure 4: Interfacing the MXene microelectrode array with the adapter board. (A) PCB with pads for soldering Omnetics and ZIF connectors. (B) PCB after soldering of Omnetics and ZIF connectors. (C) Addition of polyimide layers to back side of Au bonding pads of device, to give sufficient thickness for the ZIF connector. Two layers of polyimide are added (top) and then trimmed around the edges (bottom). (D) MXene microelectrode array inserted into the ZIF connector with proper alignment. (E) Top view of MXene microelectrode array connected to adapter board and ready for a recording experiment. Scale bars are 2 mm.

Figure 5: Representative neural recording results. (A) Illustration of placement of micro-ECOG array on cortical surface of an anesthetized rat. (B) Segment of recorded cortical activity shown for 9 electrodes. Putative cortical “down” states based on trough of the slow oscillation (1–2 Hz) are indicated by red circles. (C) Power spectral densities for each recording channel. (D) “Down” state-triggered scalogram for representative micro-ECOG channel. Note broadband power attenuation during “down” state and selective β -band (15–30 Hz) and γ -band (40–120 Hz) power amplification during “up” state. Overlaid black trace shows average slow oscillation.

DISCUSSION:

The MXene synthesis and delamination procedure described in this protocol (HF/HCl/LiCl) was built from the MILD etching approach which employed a LiF/HCl (in situ HF) etchant medium²⁶. The MILD approach allows for large Ti₃C₂ flakes (several μ m in lateral size) to be spontaneously delaminated during washing once pH ~5–6 has been attained. Compared to etching with HF

alone, this results in material with higher quality and improved material properties, such as electronic conductivity and chemical stability. The HF/HCl/LiCl method takes advantage of the MILD synthesis improvements, while additionally separating each step (etching, intercalation, and delamination) allowing for more user control.

During step 1.1, the ratio of raw materials (TiC, Al, Ti), temperature, temperature ramp rate, and time are critical to achieving the correct MAX phase. Sieving of the MAX phase prior to etching will ensure more homogenous etching. Adding the MAX phase to the etchant media (step 1.2) must be conducted slowly to prevent overheating and a general rule of 5 min per 1 g of MAX is suggested. If overheating becomes a challenge, an ice bath should be employed during addition of the Ti_3AlC_2 MAX phase. When washing the etching reaction to neutral pH (step 1.3), each acidic supernatant after centrifugation should be transparent. If the supernatant after centrifugation is dark or dilute green, increase the centrifuge time and/or speed to sediment material. Because the addition of LiCl to H_2O is exothermic, some heating will occur (step 1.4). In this procedure, the intercalation time (step 1.4) is 12 h, although it can be modified or shortened to as little as 15 minutes. The quality of delamination (step 1.5) is specific to the quantity of water used during washing and the degree of agitation. The supernatants decanted during this step may be dilute instead of transparent. If sedimentation of material becomes a challenge, increasing the centrifuge speed/rcf should be used. It is critical to perform separation and size selection by centrifugation (step 1.5) to avoid polydisperse samples. Failure to perform this step will result in an ink that has both Ti_3AlC_2 MAX phase contamination and large multilayer Ti_3C_2 particles. During step 1.6, it is important that the headspace volume of the vial is minimized.

During the fabrication of the MXene microelectrode arrays, there are several critical steps which are essential for producing functioning, high-quality electrodes. It is important to design the first photomask such that there is a metal ring patterned around the outer edge of the wafer (step 2.2) and the second photomask such that there is a corresponding, slightly larger diameter ring which will be etched through the sacrificial parylene-C (step 2.4) layer to aid in removing the sacrificial layer. Without this ring, it can be difficult to establish an edge to begin peeling up the sacrificial parylene-C layer in step 2.7. During step 2.3, it is critical to expose the wafer to O_2 plasma to allow the dilute cleaning solution to properly wet and adhere to the wafer. Failure to perform this step will result in areas of the wafer not accumulating an anti-adhesive layer, which renders the removal of the sacrificial parylene-C layer in step 2.7 impossible. During the removal of the sacrificial parylene-C layer in step 2.7, it is important to be careful to avoid scratching or damaging the bottom parylene-C layer, as this can lead to the formation of bubbles between the bottom parylene-C and the Si wafer, and subsequent delamination. If the sacrificial parylene-C layer does not peel up easily, a slightly more concentrated cleaning solution (4% in DI) can be used in step 2.3.1, or the O_2 plasma exposure in step 2.3.1 can be prolonged to improve hydrophilicity of the underlying parylene-C layer.

After the fabrication is completed, properly interfacing the MXene device with the connector board is essential. The addition of two layers of polyimide tape in step 3.2 is essential to ensure proper thickness for insertion into the ZIF connector, however care should be taken to avoid accidental folding or crumpling of the thin parylene-C device while the tape is added, as it is not

possible to remove the tape without damaging the device. Subsequently, proper alignment of the Au bonding pads on the MXene device with pins inside the ZIF connector (**Figure 4D**) is essential for forming a robust connection (step 3.3). At this stage, measuring the impedance of the MXene electrodes is helpful for troubleshooting. A 50 μm x 50 μm square MXene electrode should have an impedance magnitude near 50 k Ω at a frequency of 1 kHz in 1x PBS, and a 25 μm diameter circular MXene electrode should have an impedance magnitude near 200 k Ω under the same parameters³⁶. An impedance significantly larger than this can indicate that the electrode is not properly connected in the ZIF connector, or that the MXene electrode is not exposed, as may happen if either the top parylene-C layer was not completely etched in step 2.10 or the SiO₂ protective layer was not fully etched in step 2.11.

One limitation of this method is variability in MXene film thickness that is sometimes observed after spin-casting MXene onto the wafer. This variability can become more pronounced if electrodes are scaled up to larger areas. This limitation can be readily overcome by utilizing spray-coating instead of spin-coating to apply MXene to the wafer, representing another simple, low-cost solution processing method with which MXene, and this protocol, are compatible³⁹.

The protocol described here presents exciting new opportunities in neuroscience and in the larger field of bioelectronics. While there has long been interest in leveraging carbon-based nanomaterials for neural microelectrodes, the incorporation of Ti₃C₂ MXene into such electrodes has enabled significantly simpler and more high-throughput fabrication than has been possible with other carbon-based nanomaterials. Furthermore, the outstanding properties of Ti₃C₂ MXene endow the electrodes with remarkably low impedance for their size, thus improving sensitivity and signal quality. A growing body of literature also describes a number of methods for micropatterning MXene, which may be adapted for fabricating MXene microelectrodes in the future, including micro-contact printing⁴⁰, inkjet printing^{41,42}, and automated scalpel engraving⁴³. There exists great potential to extend this protocol to fabricate Ti₃C₂ MXene electrodes of arbitrary size and geometry for a range of biosensing applications.

ACKNOWLEDGMENTS:

This work was supported by the National Institutes of Health (grant no. R21-NS106434), the Citizens United for Research in Epilepsy Taking Flight Award, the Mirowski Family Foundation and Neil and Barbara Smit (F.V.); the National Science Foundation Graduate Research Fellowship Program (grant no. DGE-1845298 to N.D. and B.M.); the Army Research Office (Cooperative Agreement Number W911NF-18-2-0026 to K.M.); and by the U.S. Army via the Surface Science Initiative Program at the Edgewood Chemical Biological Center (PE 0601102A Project VR9 to Y.G. and K.M.). This work was carried out in part at the Singh Center for Nanotechnology, which is supported by the National Science Foundation National Nanotechnology Coordinated Infrastructure Program (NNCI-1542153).

DISCLOSURES:

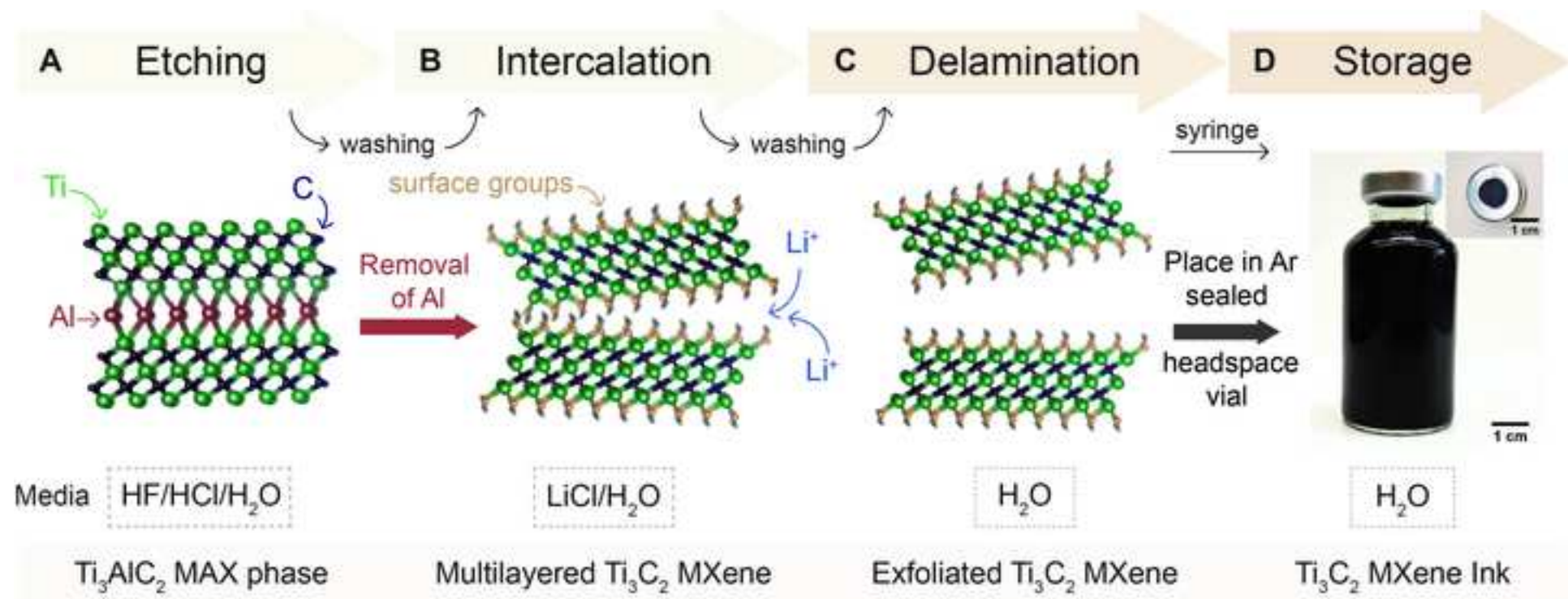
The authors have nothing to disclose.

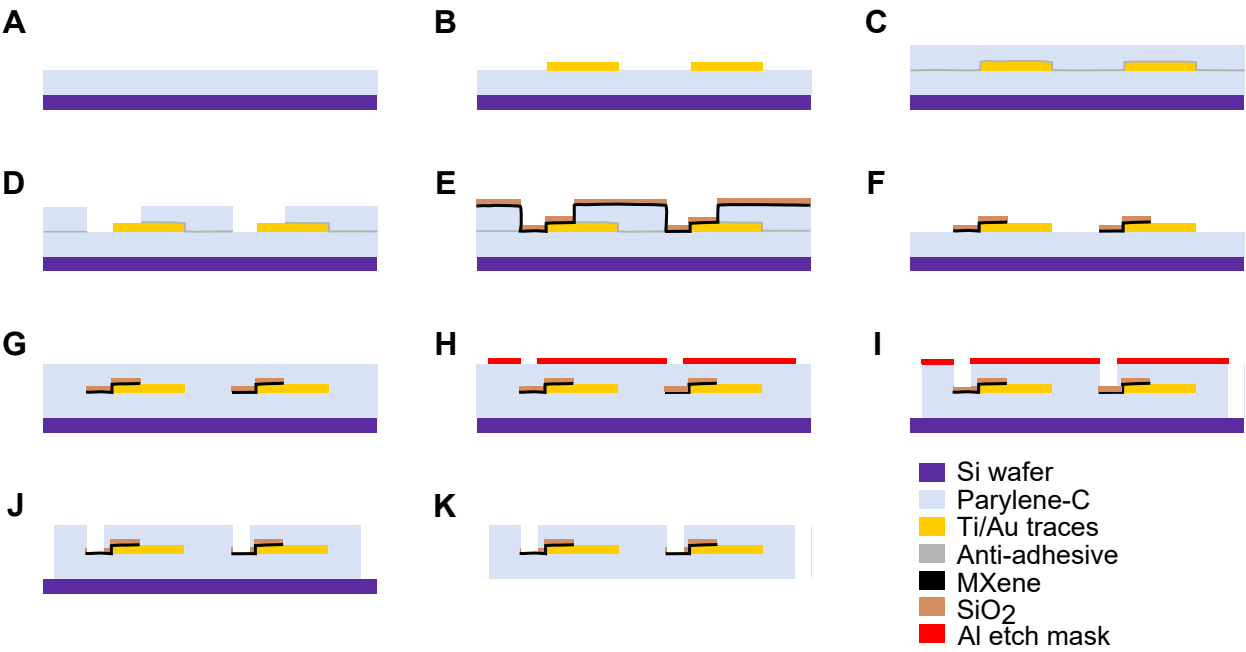
REFERENCES:

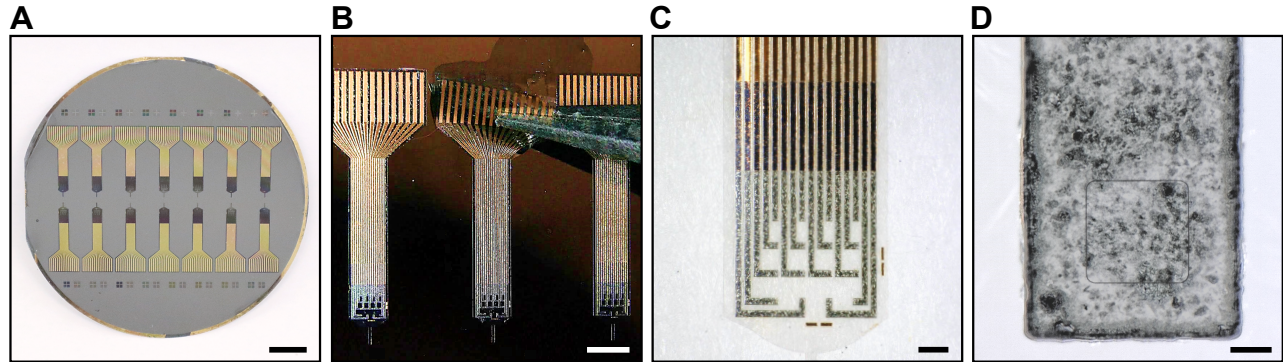
- 573 1. Ludwig, K.A. et al. Poly(3,4-ethylenedioxythiophene) (PEDOT) polymer coatings facilitate
574 smaller neural recording electrodes. *Journal of Neural Engineering*. **8** (1), 014001 (2011).
- 575 2. Polikov, V.S., Tresco, P.A., Reichert, W.M. Response of brain tissue to chronically
576 implanted neural electrodes. *Journal of Neuroscience Methods*. **148** (1), 1–18 (2005).
- 577 3. Lecomte, A., Descamps, E., Bergaud, C. A review on mechanical considerations for
578 chronically-implanted neural probes. *Journal of Neural Engineering*. **15** (3), 031001 (2017).
- 579 4. Castagnola, E. et al. Smaller, softer, lower-impedance electrodes for human
580 neuroprosthesis: a pragmatic approach. *Frontiers in Neuroengineering*. **7**, 8 (2014).
- 581 5. Nguyen, J.K. et al. Mechanically-compliant intracortical implants reduce the
582 neuroinflammatory response. *Journal of Neural Engineering*. **11** (5), 056014 (2014).
- 583 6. Boehler, C., Stieglitz, T., Asplund, M. Nanostructured platinum grass enables superior
584 impedance reduction for neural microelectrodes. *Biomaterials*. **67**, 346–353 (2015).
- 585 7. Petrossians, A., Whalen, J.J., Weiland, J.D., Mansfeld, F. Surface modification of neural
586 stimulating/recording electrodes with high surface area platinum-iridium alloy coatings. *2011*
587 *Annual International Conference of the IEEE Engineering in Medicine and Biology Society*.
588 3001–3004 (2011).
- 589 8. Meyer, R.D., Cogan, S.F., Nguyen, T.H., Rauh, R.D. Electrodeposited iridium oxide for
590 neural stimulation and recording electrodes. *IEEE Transactions on Neural Systems and*
591 *Rehabilitation Engineering*. **9** (1), 2–11 (2001).
- 592 9. Ferguson, J.E., Boldt, C., Redish, A.D. Creating low-impedance tetrodes by electroplating
593 with additives. *Sensors and Actuators A: Physical*. **156** (2), 388–393 (2009).
- 594 10. Kotov, N.A. et al. Nanomaterials for Neural Interfaces. *Advanced Materials*. **21** (40),
595 3970–4004 (2009).
- 596 11. Keefer, E.W., Botterman, B.R., Romero, M.I., Rossi, A.F., Gross, G.W. Carbon nanotube
597 coating improves neuronal recordings. *Nature Nanotechnology*. **3** (7), 434–439 (2008).
- 598 12. Lu, Y. et al. Electrodeposited polypyrrole/carbon nanotubes composite films electrodes
599 for neural interfaces. *Biomaterials*. **31** (19), 5169–5181 (2010).
- 600 13. Green, R.A., Williams, C.M., Lovell, N.H., Poole-Warren, L.A. Novel neural interface for
601 implant electrodes: improving electroactivity of polypyrrole through MWNT incorporation.
602 *Journal of Materials Science: Materials in Medicine*. **19** (4), 1625–1629 (2008).
- 603 14. Apollo, N. V. et al. Soft, Flexible Freestanding Neural Stimulation and Recording Electrodes
604 Fabricated from Reduced Graphene Oxide. *Advanced Functional Materials*. **25** (23), 3551–3559
605 (2015).
- 606 15. Lu, Y., Lyu, H., Richardson, A.G., Lucas, T.H., Kuzum, D. Flexible Neural Electrode Array
607 Based-on Porous Graphene for Cortical Microstimulation and Sensing. *Scientific Reports*. **6** (1),
608 33526 (2016).
- 609 16. Matarredona, O. et al. Dispersion of Single-Walled Carbon Nanotubes in Aqueous
610 Solutions of the Anionic Surfactant NaDDBS. *The Journal of Physical Chemistry B*. **107** (48),
611 13357–13367 (2003).
- 612 17. Ramesh, S. et al. Dissolution of Pristine Single Walled Carbon Nanotubes in Superacids by
613 Direct Protonation. *The Journal of Physical Chemistry B*. **108** (26), 8794–8798 (2004).
- 614 18. Kim, S.W. et al. Surface modifications for the effective dispersion of carbon nanotubes in
615 solvents and polymers. *Carbon*. **50** (1), 3–33 (2012).
- 616 19. Wang, M. et al. Nanotechnology and Nanomaterials for Improving Neural Interfaces.

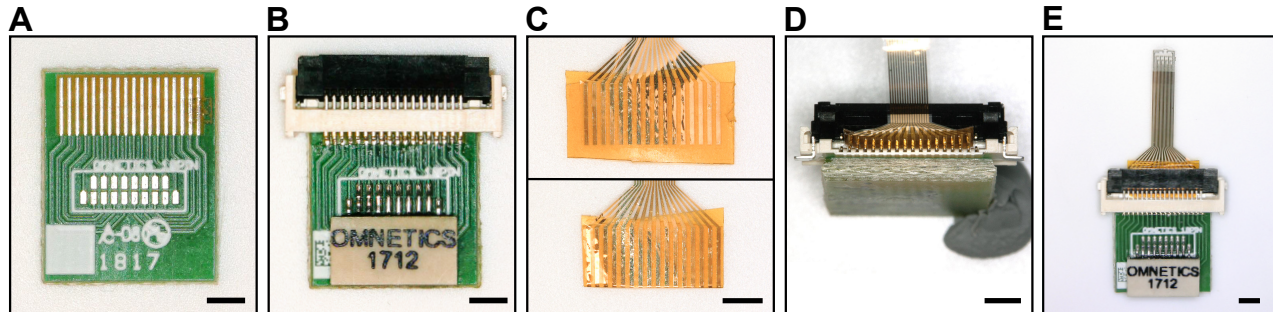
- Advanced Functional Materials*. **28** (12), 1700905, (2017).
20. Wang, K., Fishman, H.A., Dai, H., Harris, J.S. Neural Stimulation with a Carbon Nanotube Microelectrode Array. *Nano Letters*. **6** (9), 2043–2048 (2006).
21. Ansaldo, A., Castagnola, E., Maggiolini, E., Fadiga, L., Ricci, D. Superior Electrochemical Performance of Carbon Nanotubes Directly Grown on Sharp Microelectrodes. *ACS Nano*. **5** (3), 2206–2214 (2011).
22. Nimbalkar, S. et al. Ultra-Capacitive Carbon Neural Probe Allows Simultaneous Long-Term Electrical Stimulations and High-Resolution Neurotransmitter Detection. *Scientific Reports*. **8**, 6958 (2018).
23. Anasori, B., Lukatskaya, M., Gogotsi, Y. 2D metal carbides and nitrides (MXenes) for energy storage. *Nature Reviews Materials*. **2**, 16098 (2017).
24. Anasori, B., Gogotsi, Y. *2D Metal Carbides and Nitrides (MXenes): Structure, Properties and Applications*. Springer Nature. Switzerland (2019).
25. Naguib, M. et al. Two-Dimensional Nanocrystals Produced by Exfoliation of Ti_3AlC_2 . *Advanced Materials*. **23** (37), 4248–4253 (2011).
26. Alhabeb, M. et al. Guidelines for Synthesis and Processing of Two-Dimensional Titanium Carbide ($\text{Ti}_3\text{C}_2\text{T}_x$ MXene). *Chemistry of Materials*. **29** (18), 7633–7644 (2017).
27. Ghidui, M., Lukatskaya, M.R., Zhao, M.-Q., Gogotsi, Y., Barsoum, M.W. Conductive two-dimensional titanium carbide ‘clay’ with high volumetric capacitance. *Nature*. **516** (7529), 78–81 (2014).
28. Lukatskaya, M.R. et al. Ultra-high-rate pseudocapacitive energy storage in two-dimensional transition metal carbides. *Nature Energy*. **2**, 17105 (2017).
29. Zhu, Y. et al. Carbon-Based Supercapacitors Produced by Activation of Graphene. *Science*. **332** (6037), 1537–1541 (2011).
30. Heon, M. et al. Continuous carbide-derived carbon films with high volumetric capacitance. *Energy & Environmental Science*. **4** (1), 135–138 (2011).
31. Yang, X., Cheng, C., Wang, Y., Qiu, L., Li, D. Liquid-mediated dense integration of graphene materials for compact capacitive energy storage. *Science*. **341** (6145), 534–7 (2013).
32. Zhang, C.J. et al. Transparent, Flexible, and Conductive 2D Titanium Carbide (MXene) Films with High Volumetric Capacitance. *Advanced Materials*. **29** (36), 1702678 (2017).
33. Han, X. et al. 2D Ultrathin MXene-Based Drug-Delivery NanoplatforM for Synergistic Photothermal Ablation and Chemotherapy of Cancer. *Advanced Healthcare Materials*. **7** (9), 1701394 (2018).
34. Dai, C. et al. Biocompatible 2D Titanium Carbide (MXenes) Composite Nanosheets for pH-Responsive MRI-Guided Tumor Hyperthermia. *Chemistry of Materials*. **29** (20), 8637–8652 (2017).
35. Xu, B. et al. Ultrathin MXene-Micropattern-Based Field-Effect Transistor for Probing Neural Activity. *Advanced Materials*. **28** (17), 3333–3339 (2016).
36. Driscoll, N. et al. Two-Dimensional Ti_3C_2 MXene for High-Resolution Neural Interfaces. *ACS Nano*. **12** (10), 10419–10429 (2018).
37. Sessolo, M. et al. Easy-to-Fabricate Conducting Polymer Microelectrode Arrays. *Advanced Materials*. **25** (15), 2135–2139 (2013).
38. Shuck, C.E. et al. Effect of Ti_3AlC_2 MAX Phase on Structure and Properties of Resultant $\text{Ti}_3\text{C}_2\text{T}_x$ MXene. *ACS Applied Nano Materials*. **2** (6), 3368–3376 (2019).

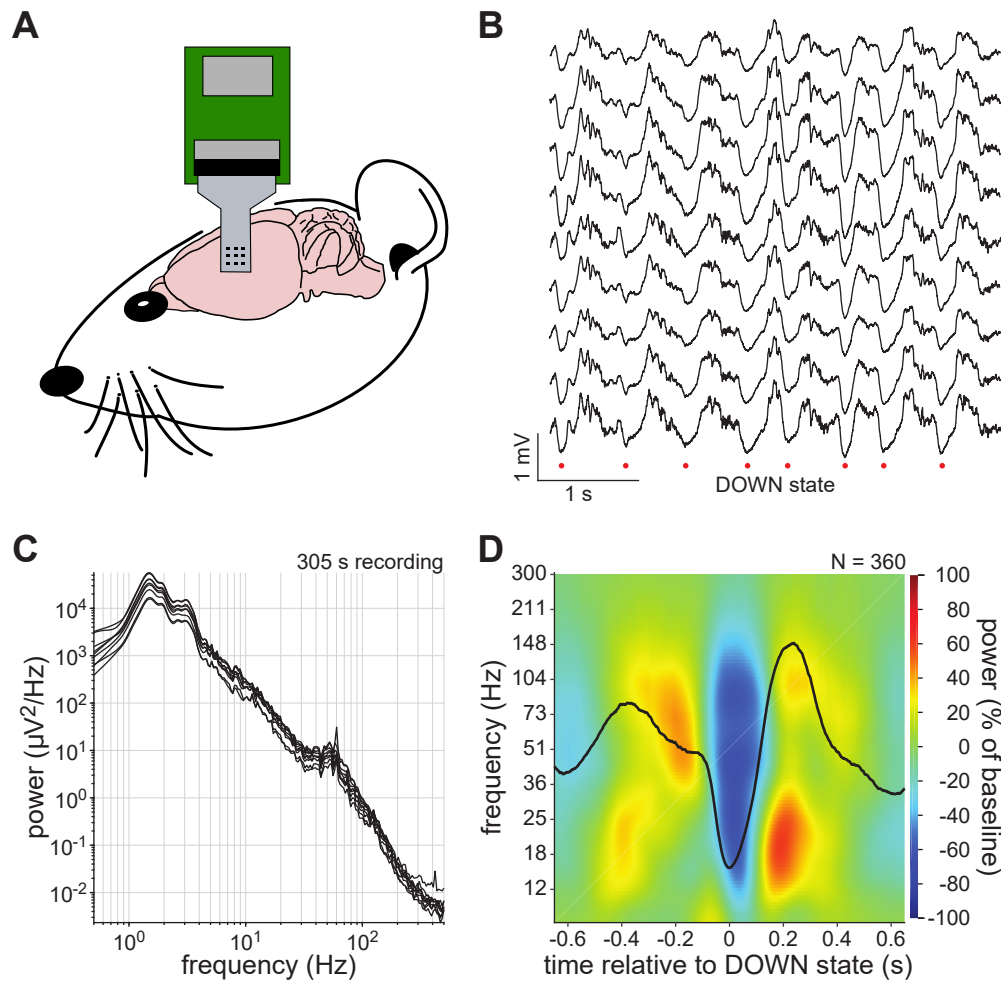
- 661 39. Hantanasirisakul, K. et al. Fabrication of $\text{Ti}_3\text{C}_2\text{T}_x$ MXene Transparent Thin Films with
662 Tunable Optoelectronic Properties. *Advanced Electronic Materials*. **2** (6), 1600050 (2016).
- 663 40. Xu, B. et al. Ultrathin MXene-Micropattern-Based Field-Effect Transistor for Probing
664 Neural Activity. *Advanced Materials*. **28** (17), 3333–3339 (2016).
- 665 41. Zhang, C. et al. Additive-free MXene inks and direct printing of micro-supercapacitors.
666 *Nature Communications*. **10** (1), 1795 (2019).
- 667 42. Quain, E. et al. Direct Writing of Additive-Free MXene-in-Water Ink for Electronics and
668 Energy Storage. *Advanced Materials Technologies*. **4** (1), 1800256 (2019).
- 669 43. Salles, P., Quain, E., Kurra, N., Sarycheva, A., Gogotsi, Y. Automated Scalpel Patterning of
670 Solution Processed Thin Films for Fabrication of Transparent MXene Microsupercapacitors.
671 *Small*. **14** (44), 1802864 (2018).
- 672











Name of Reagent/ Equipment	Company	Catalog Number	Comments/Description
00-90 screw	McMaster-Carr	90910A630	Skull screw around which ground wire is wrapped
128ch stimulation/recording controller	Intan Technologies		A component of the neural recording system.
175 mL polypropylene (PP) conical centrifuge tubes	Falcon	REF: 352076	Used for washing
18 position 0.5 mm pitch ZIF connector	Molex	505110-1892	Used to interface the flexible Parylene microelectrod
18 position dual row male nano-miniature (.025"/.64mm) connector	Omnetics Connector Corporation	A79008-001	Used to interface the PCB adapter board to the recor
3ML Disposable Plastic Set Transfer Graduated Pipettes	Rienar	Rienar-3ML-20PCS	Used for transferring etchant or MXene solutions
50 mL polyproylene (PP) conical centrifuge tube	Falcon	REF: 352070	Used for washing and size selection
Al etchant Type A	Transene	060-0026000-QT	For removing Al etch mask layer after final Parylene-co
Aluminum Powder, -325 Mesh, 99.5% (metals basis), particle size < 44 µm	Alfa Aesar	CAS: 7429-90-5	Used for MAX synthesis
AutoCAD software	Autodesk Inc.		Design software for drawing photomasks. Free alterr
Buffered Oxide Etchant 6:1	JT Baker Wildlife	1178-03	For removing SiO ₂ layer to expose MXene electrode c
Buprenorphine SR	Pharmaceuticals		Analgesia for rat surgery
Centrifuge	Hermle	Benchmark Z 446	Used for washing and size selection
	Midwest Veterinary		
Dexdomitor	Supply	193.13250.3	Anesthesia for rat surgery
Drill burr	Fine Science Tools	19007-07	Burrs for drill
Electric drill	Foredom	K.1070	Micromotor drill for craniotomies
Electron beam evaporator	Kurt J. Lesker Company		Used to evaporate Ti, Au, and SiO ₂ during fabrication
Ground wire	A-M Systems	781500	Bare silver wire

Headspace Vial, glass	Supelco	REF: 27298	Used for storing MXene solutions
Hydrochloric acid (12.1N)	Fisher Scientific	CAS: 7647-01-0	Corrosive; etchant material
Hydrofluoric Acid, (48-51% solution in H ₂ O)	Acros	CAS: 7664-39-3	Etchant material
Jupiter II RIE system	March Plasma Systems Inc.		Planar RIE etching system used to etch the Parylene-C
Kapton standard polyimide tape, 1/4"	DuPont		Used to add thickness to the Au bonding pad region
Ketamine	Hospital of the Univ. of Penn.		Anesthesia for rat surgery
KLA P-7 Stylus Profilometer	KLA Corporation		Used to measure 2D profiles to confirm complete etch
Lithium chloride, 99% for analysis, anhydrous	Acros	CAS: 7447-41-8	Hygroscopic; delamination material
MA6 mask aligner	Karl Suss Microtec AG International Products Corporation		Used to align each photomask to the pattern on the wafer
Micro-90 cleaning solution	Futurrex Inc.	M-9050-12	Used as the anti-adhesive layer to enable removal of
NR71-3000p photoresist	Midwest Veterinary Supply	NR71-3000p	Negative photoresist used to define Ti/Au traces and
Ophthalmic ointment	Specialty Coating Systems	193.63200.3	To prevent corneal drying during surgery
Parylene deposition system	Specialty Coating Systems		Used to evaporate thin conformal films of Parylene-C
Parylene-C dimer	Specialty Coating Systems	980130-c-01lbe	Flexible polymer used as bottom and top passivating
Photomasks (chrome on soda lime glass)	University of Pennsylvania		Our photomasks were produced in the University cleanroom
Povidone-iodine solution	Medline	MDS093901	To help prevent infection around scalp incision
Printed Circuit Board (PCB)	Advanced Circuits		Used to interface between the MXene electrode array and the amplifier
RD6 Developer	Futurrex Inc.	RD6 Developer	Used to develop NR71-3000p negative photoresist for lithography
Reference 600 potentiostat	Gamry Instruments		Used to measure the electrodes' impedance to assess electrode quality
Remover PG	MicroChem Corp.	G050200	Used to remove NR71-3000p following metal deposition
RHS2000 Stim SPI interface cable	Intan Technologies		A component of the neural recording system.
RHS2116 amplifier board	Intan Technologies		A component of the neural recording system.

Si wafers	Wafer World	2885	Substrate for fabrication
Spin Coater	Cost Effective		
Stereotaxic frame	Equipment		For coating wafers with resists and applying the Micr
Teflon-coated magnetic stir bar	Kopf Instruments	Model 902	For positioning the rat for neurosurgery
Titanium carbide, 99.5% (metals basis), particle size ~2 µm	Corning	REF: 1233W95	Used to stir during etching and intercalation
	Alfa Aesar	CAS: 12070-08-5	Used for MAX synthesis
Titanium powder, -325 mesh, 99% (metals basis), particle size < 44µm	Alfa Aesar	CAS: 7440-32-6	Used for MAX synthesis
Ultrasonic bath sonicator	Reynolds Tech		For removing metal and photoresist particles during
UV vis spectrophotometer	ThermoScientific	Evolution 201	Used to determine concentration and observe absorp
Zetasizer, Particle Size Analysis	Malvern Panalytical	Nano ZS	Used to determine particle lateral size distibution

le array with the PCB adapter board.

rding headstage.

C etch.

atives include DraftSight and LayoutEditor.
contacts at the end of the fabrication procedure.

1. Most university clean rooms have this or a similar tool.

C using O₂ plasma. Most university clean rooms have a comparable planar RIE etching system.

of the flexible Parylene microelectrode array for insertion into the ZIF connector.

etching through the sacrificial parylene-C layer in step 2.4.2. Most university clean rooms have this or a comparable stylus profilometer to

wafer and expose the wafer to UV light. Most university clean rooms have this or a similar tool.

the sacrificial Parylene-C layer to pattern the MXene
MXene patterns in the devices.

2

layers for the flexible MXene devices

an room using a Heidelberg DWL66+ laser writer system, however several vendors manufacture photomasks from provided design files.

ry and the measurement electronics such as the potentiostat and the Intan recording system. Advanced Circuits and other vendors manuf
ollowing UV exposure
is quality of the devices
tion to perform lift-off patterning

Mo-90 and MXene layers. Most university clean rooms have spin coaters.

lift-off processes to pattern metals.

Optical peak

ol.

facture and assemble PCBs based on the provided design files.

Manuscript JoVE60741: Fabrication of Ti3C2 MXene microelectrode arrays for in vivo neural recording

Authors: Nicolette Driscoll, Kathleen Maleski, Andrew G. Richardson, Brendan Murphy, Babak Anasori, Timothy H. Lucas, Yury Gogotsi, and Flavia Vitale

Response to Editorial and Reviewer Comments

We thank the Editors and reviewers for their insightful comments. We would like to particularly thank all the reviewers for their kind words of appreciation for our work.

We have addressed all of the comments in the revised version of the manuscript and tracked them with the document review mode.

Below we address the comments individually. Our responses are marked in **bold**.

Editorial Comments:

1. Please take this opportunity to thoroughly proofread the manuscript to ensure that there are no spelling or grammar issues. The JoVE editor will not copy-edit your manuscript and any errors in the submitted revision may be present in the published version.

The authors have thoroughly proofread the manuscript.

2. Please revise lines 96-106, 108-109, 119-122, 125-129, and 456-460 to avoid textual overlap with previously published work.

The authors have revised the highlighted lines of text in the attempt to avoid overlap with previously published works. Please note that lines 96-106 and 108-109 contain factual descriptions of MXene and some overlap might be unavoidable.

3. Keywords: Please provide at least 6 keywords or phrases.

The authors have added the additional keywords “nanomaterials” and “neuroengineering.”

4. Please revise the Protocol to contain only action items that direct the reader to do something (e.g., “Do this,” “Ensure that,” etc.). The actions should be described in the imperative tense in complete sentences wherever possible. Avoid usage of phrases such as “could be,” “should be,” and “would be” throughout the Protocol. Any text that cannot be written in the imperative tense may be added as a “NOTE.” Please include all safety procedures and use of hoods, etc. However, notes should be used sparingly and actions should be described in the imperative tense wherever possible. Please move the discussion about the protocol to the Discussion.

The protocol has been revised to contain only action items described in imperative tense, and additional text has been moved to a “NOTE” where relevant. In particular, step 1.1 was revised to describe actions in imperative tense. Safety precautions and use of hoods are included in “NOTE” and “CAUTION” statements at the beginning of each section of the protocol.

5. The Protocol should be made up almost entirely of discrete steps without large paragraphs of text between sections. Please simplify the Protocol so that individual steps contain only 2-3 actions per step and a maximum of 4 sentences per step. Use sub-steps as necessary.

The protocol has been revised so that individual steps contain only 2-3 actions per step and a maximum of 4 sentences per step. In particular, step 1.5 has been broken up into sub-steps to avoid a large paragraph of text.

6. 4.3: Please specify the age, gender and type of rat used. Please mention how proper anesthetization is confirmed.

The authors have added details to specify using adult male Sprague Dawley rats, and rephrased the instructions describing how to monitor proper level of anesthetization (added step 4.3).

7. Please include single line spacing between each numbered step or note in the protocol.

Single line spacing has been added between each main step in the protocol.

8. After you have made all the recommended changes to your protocol section (listed above), please highlight in yellow up to 2.75 pages (no less than 1 page) of protocol text (including headers and spacing) to be featured in the video. Bear in mind the goal of the protocol and highlight the critical steps to be filmed. Our scriptwriters will derive the video script directly from the highlighted text.

Done.

9. Please highlight complete sentences (not parts of sentences). Please ensure that the highlighted steps form a cohesive narrative with a logical flow from one highlighted step to the next. The highlighted text must include at least one action that is written in the imperative voice per step. Notes cannot usually be filmed and should be excluded from the highlighting.

Done.

10. Please include all relevant details that are required to perform the step in the highlighting. For example: If step 2.5 is highlighted for filming and the details of how to perform the step are given in steps 2.5.1 and 2.5.2, then the sub-steps where the details are provided must be highlighted.

Done.

11. Please remove the embedded figure(s) from the manuscript.

The embedded figures have been removed from the manuscript.

12. Table of Materials: Please sort the materials alphabetically by material name.

The materials have been sorted alphabetically by material name.

Reviewers' comments:

Reviewer #1:

Manuscript Summary:

This manuscript describes a methodology for fabricating Ti₃C₂ MXene microelectrode arrays and using them for in vivo micro-electrocorticography recording.

More specifically, the presented protocol describes a novel method for micropatterning Ti₃C₂ MXene into microelectrode arrays on flexible polymeric substrates, enables simple and scalable fabrication of microelectrodes from solution-based conductive inks.

The paper is well written, and the methodology is clearly detailed.

Minor comments:

Lines 77-82

'effective surface area' of the electrode. This can be achieved through nanopatterning, surface roughening, or electroplating with porous additives..... For example, carbon nanotubes have been used as a coating to significantly reduce electrode impedance'

The following papers can be cited to further support this argument:

Lu, Y.; et al. Electrodeposited Polypyrrole/Carbon Nanotubes Composite Films Electrodes for Neural Interfaces. *Biomaterials*, 31, 5169-518, 2010

Green, R. A.; Williams, C. M.; Lovell, N. H.; Poole-Warren, L. A. Novel Neural Interface for Implant Electrodes: Improving Electroactivity of Polypyrrole through MWNT Incorporation. *J. Mater. Sci.: Mater. Med.*, 19, 1625- 1629, 2008.

Line 90,

The following papers can be cited to further support this argument:

chemical vapor deposition (CVD), typically require high temperatures which are incompatible with many polymeric substrates

Wang, K.; Fishman, H. A.; Dai, H.; Harris, J. S. Neural Stimulation with a Carbon Nanotube Microelectrode Array. *Nano Lett.* 6, 2043-2048, 2006.

A. Ansaldo, et al. Superior electrochemical performance of carbon nanotubes directly grown on sharp microelectrodes, *ACS nano* 5 (3), 2206-2214, 2011

S Nimbalkar, et al., Ultra-capacitive carbon neural probe allows simultaneous long-term electrical stimulations and high-resolution neurotransmitter detection, *Scientific reports* 8 (1), 6958, 2018

The authors thank the reviewer for the helpful comments and insightful suggestions. We have added all of the suggested citations to the introduction to further support our arguments.